

Investigation of the dielectric properties of polymer-dispersive liquid-crystal films doped with silicon dioxide nanoparticles

© T.A. Chimytov,^{1,2} A.V. Nomoev,^{1,2} D.Zh. Bazarova,^{2,3} S.V. Kalashnikov^{1,2}

¹Physical Material Science Institute, Siberian Branch, Russian Academy of Sciences, 670047 Ulan-Ude, Russia

²Banzarov Buryat State University, 670000 Ulan-Ude, Russia

³Physical Material Science Institute, Siberian Branch, Russian Academy of Sciences, 670000 Ulan-Ude, Russia

e-mail: ars-d@mail.ru

Received January 17, 2023

Revised July 28, 2023

Accepted August 25, 2023

In this work, a measuring system was developed according to the scheme of an AC bridge, with the help of which a constant voltage was applied to polymer-dispersed liquid-crystal films doped with silicon dioxide nanoparticles. For these cells with different content of silicon dioxide nanoparticles, capacitance-voltage measurements were carried out at different frequencies of the alternating voltage generator. For these cells, a memory effect was found, which manifests itself in the hysteresis behavior of the capacitance of these cells. The largest hysteresis area and the largest shift of the cell capacitance in the absence of an external field are observed at 10 kHz. In the entire region under study, with a minimum at a frequency of 10 kHz, the perpendicular component of the permittivity has a pronounced dispersion. It has been established that the content of silicon dioxide nanoparticles affects the permittivity of a polymer-dispersed liquid-crystal cell. The data obtained can be used in the development of energy-independent nanostructured data storage systems.

Keywords: polymer-dispersed liquid crystal films, silicon dioxide nanoparticles, memory effect, capacitance-voltage characteristic, dispersion.

DOI: 10.61011/TP.2023.10.57450.7-23

Introduction

Recently, the studies in the field of physics of polymer-dispersed liquid crystal (PDLC) films doped, in particular, with various nanoparticles [1,2] have aroused a great interest. Such materials have, on the one hand, unique properties of liquid crystals (LC), as well as mechanical elastic properties due to structural reinforcement by polymers.

It was found in the study of PDLC films with BaTiO₃ and ZnO ferroelectric nanoparticles that the addition of such nanoparticles reduces the threshold voltage and saturation voltage by 85 and 41%, respectively, due to spontaneous polarization of ferroelectric nanoparticles [3]. It was shown in [4,5] that even a small quantity of BaTiO₃ ferroelectric nanoparticles in nematic LC causes a sufficiently strong electromechanical memory effect, which manifests itself in the hysteresis behavior of dielectric characteristics. In addition, it was shown that the introduction of nanoparticles improves the electro-optical properties of LC, which in the future leads to energy efficiency of such systems. Nematic LC doped with silicon dioxide nanoparticles (SiO₂) also have a memory effect at various concentrations [6]. The authors explain the occurrence of this effect by the formation of a lattice of agglomerates of nanoparticles, in the cells of which LC molecules are packed. If such a lattice were not formed, then the LC molecules would first

line up along the field when the external field is switched on and off sequentially and then they would freely return to their original position when it is turned off like in pure, undoped LC. Thus, the dielectric permittivity of the entire volume of the LC, which depends on the directionality (director) of its molecules, would also take the initial value, and it would not be possible to detect whether the liquid crystal system was exposed to any external (electrical) impact. However, the cellular structure of the network of nanoparticle agglomerates prevents the LC molecules from returning to their initial state after the sequential switching on and off of the external field, which leads to a shift in the value of the dielectric constant (upward). The memory effect is attributable to this displacement. It should be noted that the creation of programmable storage devices based on such liquid crystal systems opens up broad prospects in multi-level data storage systems.

This paper presents the results of an experimental study of the dielectric properties of PDLC films based on nematic LC doped with SiO₂ nanoparticles.

1. Experimental equipment

Polymer (polyvinyl acetate) and nematic LC are used as materials for creating a PDLC film. An additive of SiO₂ nanopowder is added to the LC volume (0.1 or 1 wt%;

the concentration is given in mass fractions of the polymer mass). The choice of such concentrations of nanopowder in the IC is attributable to the conclusions of [6], according to which the maximum memory effect is achieved at a value of 1 wt%. „Liquid crystal–polymer “ phase separation occurs after polymerization of polyvinyl acetate resulting in the formation of a film containing LC drops. The PDLC film is clamped between two conductive (indium-tin oxide-coated) glasses, forming a dielectric cell. The thickness of the film is fixed by calibrated nylon fishing filaments with a diameter of 60 μm .

A liquid crystal widely used in various studies from a series of alkyl cyanobiphenyls 4-n-pentil-4'-cyanobiphenyl (5CB) with chemical formula $\text{C}_{18}\text{H}_{19}\text{N}$ was used in this paper as an LC. The transition from the solid crystalline state to the nematic phase for this LC takes places at a temperature of 18°C, and from the nematic to the isotropic state — at 35°C, which is accompanied by optical illumination. These crystals are thermotropic, characterized by positive dielectric anisotropy $\Delta\epsilon$ and homeotropic axis orientation. In this case, the long axes of LC molecules with a longitudinal dipole moment are located along the direction of the field perpendicular to the cell surface.

Nanopowder SiO_2 is produced by gas-phase synthesis; heating source — relativistic electron accelerator [7]. Average particle size 28.4 nm; specific surface area 96 m^2/kg ; powder density 2.2 g/cm^3 . Figure 1 shows an image of nanoparticles obtained using atomic force microscopy (scanning probe microscope SOLVER Next NT-MDT). The image shows that the nanoparticles have a spherical shape and form agglomerates of various structures.

Within the framework of this study, volt-farad measurements of the PDLC of cells were carried out. A measuring system was developed for these purposes that operates using an AC Schering bridge with the possibility of applying a constant bias voltage to the PDLC cell [8].

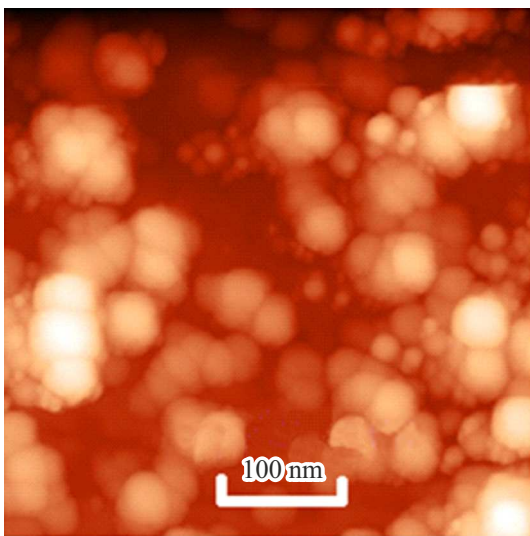


Figure 1. Image of SiO_2 nanoparticles obtained on a scanning probe microscope.

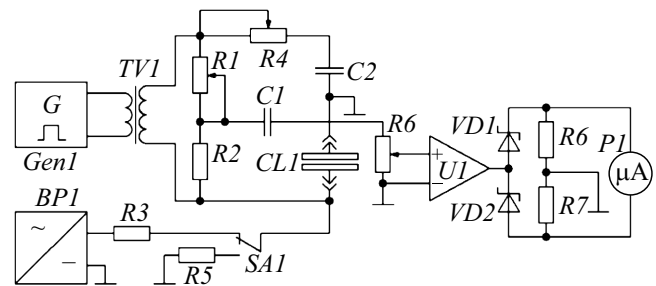


Figure 2. Simplified schematic diagram of an AC bridge with a constant offset. See text for explanations.

A simplified diagram of the AC bridge is shown in Fig. 2. The bridge is powered by alternating current from the generator *Gen1* by means of a transformer *TV1*. The bridge arms are made up of elements *R1–R3*, *C2* and PDLC cells *CL1*. The bridge is balanced by a variable resistor *R1*. The reference capacitor of the bridge *C2* is precision, a variable resistor *R4* connected in series to it allows balancing the bridge relative to the dielectric losses in the PDLC cell, which allows counting the tangent of the dielectric loss angle.

Like many liquid dielectrics, even well-purified liquid crystals have a noticeable ionic conductivity [9], which leads to the accumulation of electric charges and their relaxation near the electrodes, which can impair the quality of the cell and the accuracy of measuring its capacity.

An amplifier *U1*, a rectifier *VD1–VD2–R6–R7* and a microammeter *PI* are used as a zero indicator that provides values for balancing the bridge. The use of a two-half-period rectifier based on Schottky diodes with the replacement of two arms with resistors allows minimizing the voltage drop and, accordingly, increasing the sensitivity of the null-indicating instrument. A constant offset is applied from the regulated current source *BPI* via a resistor *R3* for measuring the parallel component of the dielectric constant to a liquid crystal cell *CL1*. This resistor is necessary to significantly increase the internal resistance of the DC source in order to reduce its effect on the equilibrium of the bridge. A resistor *R5* is connected in parallel to a liquid crystal cell for measuring the normal component of the permittivity, instead of a current source by a switch *SA1*, whose resistance is equal to the internal resistance of the source and the resistance of the resistor *R3*. Thus, when measuring both components of the dielectric constant, the same resistance is connected in parallel to the cell, which avoids distortion in the bridge reading when switching measurement modes. The capacitor *C1* prevents the zero constant offset indicator from entering the input of the amplifier, the sensitivity of the amplifier is regulated by a variable resistor *R6*. The amplifier is powered by a separate current source to prevent any parasitic circuits.

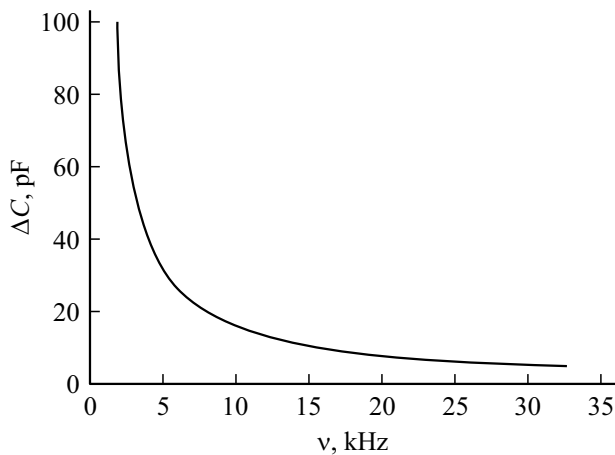


Figure 3. Dependence of the capacitance determination error ΔC on the current frequency ν .

The equilibrium condition of the considered bridge circuit can be expressed as follows:

$$\frac{1/\omega C_{L1}}{1/\omega C_2} = \frac{R_1}{R_2},$$

$$\frac{R_{3,5}/(\omega C_{L1}R_{3,5} + 1)}{1/\omega C_2} = \frac{R_1}{R_2} \Rightarrow \frac{\omega C_2 R_{3,5}}{\omega C_{L1}R_{3,5} + 1} = \frac{R_2}{R_1},$$

where $R_{3,5}$ — resistor resistance $R3$ or $R5$ connected in parallel to the measured cell. It can be seen from this formula that the capacity of the PDLC of the cell in the case of its parallelization by the active circuit depends on the frequency of the current at which the bridge operates. Therefore, if the bridge scale is graded linearly, then when measuring the dependence of the cell capacity on the frequency, an error will occur, determined by the second term. Graphically, the value of this deviation in determining the capacitance ΔC for a real bridge, depending on the value of its power supply frequency, is shown in Fig. 3. This dependence can be taken as linear and relatively insignificant only in a separate frequency range (from ~ 10 kHz). It can be argued based on the capacity of a typical laboratory PDLC cell that the error is no more than 2–5%. It is worth noting that either the difference in capacitances (dielectric anisotropy) or their ratio at different values of bias voltages [6] are most often in demand, which allows shifting the measurement range towards a lower frequency (up to 1, kHz) without compromising accuracy.

The bridge is indexed taking into account the active resistance and capacitance of the wires leading to the PDLC cell, as well as contacts. The limits of measuring the capacity of the cell are 100–500 pF, the tangent of the loss angle up to 0.05, the maximum applied constant electric displacement to the cell up to 320 V.

The measurements were carried out at different frequencies of the alternating voltage generator feeding the bridge. As a result, two sets of data were obtained on the dependence of the capacity of PDLC cell on the voltage in

Area of the hysteresis loop

Generator frequency, kHz	Σ, V (hysteresis area)	
	0.1 wt%	1 wt%
5	5.6	8.0
10	10.5	18.5
15	8.5	16.4
20	8.1	15.5
25	2.9	9.2

the frequency range of the generator 5–25 kHz for „large“ and „small“ nanoparticle concentrations (1 and 0.1 wt%).

2. Findings and discussion

Figure 4 shows graphs of the dependence of the cell capacity on the applied bias voltage with 0.1 wt% silicon dioxide content at generator frequencies 5, 10, 15, 20 and 25 kHz. The vertical scale is normalized to the initial value of the cell's PDLC capacity without an applied bias voltage: $(C - C_0)/C_0$, where C — current capacitance, C_0 — initial capacitance at zero bias voltage. The arrows on the graph indicate the directions of capacitance measurement: the lower curve is obtained, as a rule, with an increase of voltage, and the upper — with a decrease.

It can be seen that for all the considered frequencies of the generator, the volt-farad characteristic of the cells has a pronounced hysteresis behavior. When the system returns to its initial state (in the absence of voltage), the residual capacity of the cell is slightly shifted relative to the initial value. The capacity does not change for a long period of time. Heating of the sample to temperatures exceeding the temperature of the LC phase transition (35°C for 5CB) is one of the methods „to reset“ capacity to the initial value. The largest increase of capacity is observed after measurement at a frequency of 10 kHz. The residual capacity of the cell at this frequency is greater than the initial value by 13%, while at other frequencies it is about 5%.

Figure 5 shows similar measurements for a cell with a 1 wt% content of silicon dioxide in a PDLC cell.

It is worth noting that the hysteresis area for this cell is significantly larger than for a cell with a „small“ concentration of silicon dioxide. The largest increase of capacity, as in the previous case, is observed after measurement at a frequency of 10 kHz — by 8%, the increase at other frequencies is about 5%.

The following table shows the values of the areas (Σ) of the hysteresis loops for two values of silicon dioxide concentrations in the PDLC cell.

The maximum value of the hysteresis area is reached in both cases at a frequency of 10 kHz, which is consistent with the fact that the maximum displacement of the residual capacitance is also observed at this frequency. Figure 6 shows a diagram based on the data from the table for clarity.

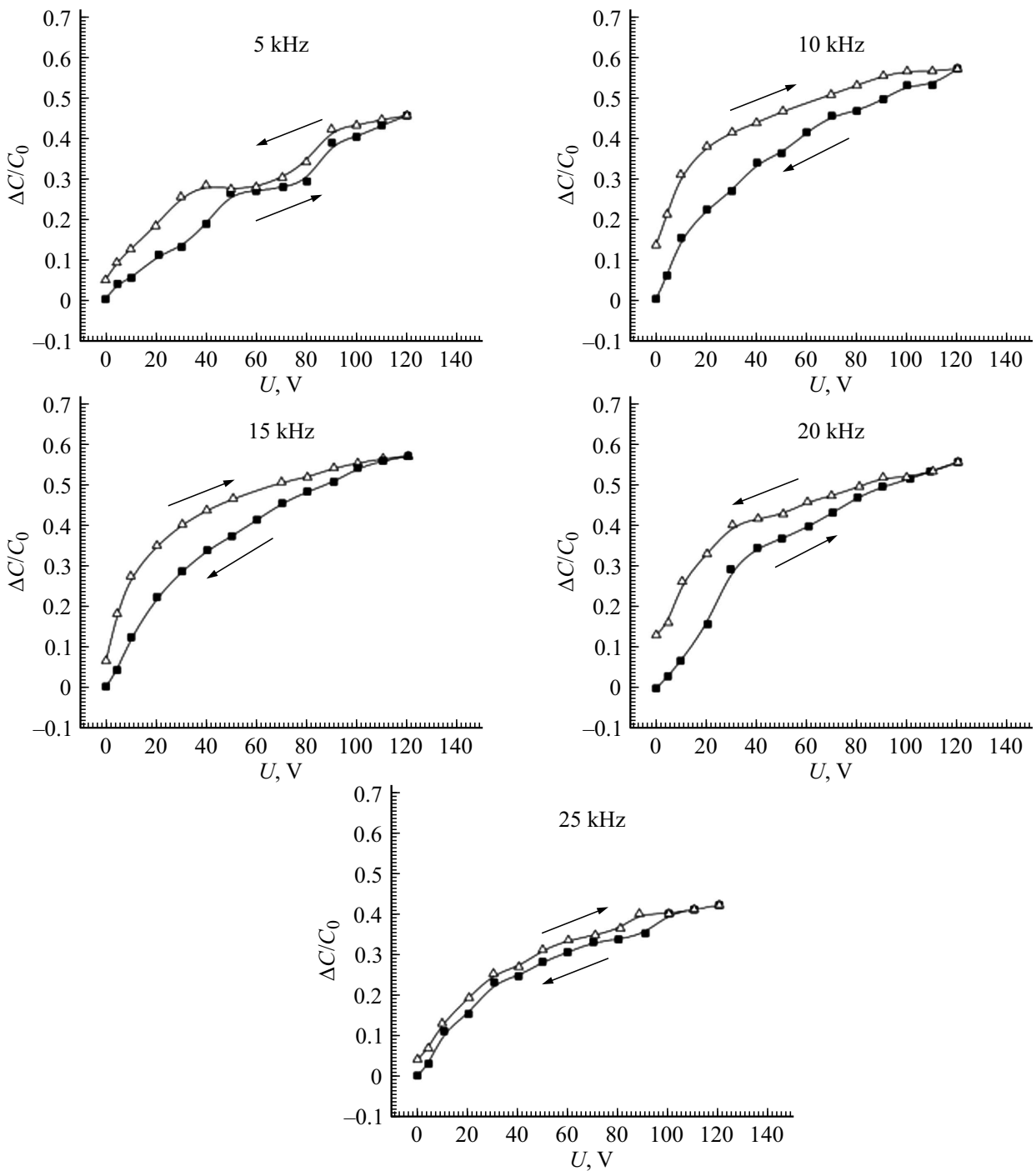


Figure 4. Volt-farad characteristics of the PDLC cell (0.1 wt% silicon dioxide) at generator frequencies 5, 10, 15, 20 and 25 kHz.

Fig. 7 shows the frequency dependences of PDLC cell capacities. Capacities are given in absolute values (pF). Lines corresponding to C_0 , — initial capacitances (before measurements); C_0^* — residual capacitances (without voltage, after volt-farad measurements).

The frequency dependence of the capacitance indicates the dispersion of the permittivity for PDLC cells with silicon dioxide, namely the perpendicular ϵ_{\perp} component, since $C_0 = \epsilon_{\perp} \epsilon_0 S/d$, where S and d — area and the

thickness of the PDLC film, respectively. At the same time, the minimum of variance is at a frequency of 10 kHz, which corresponds to the maximum memory effect for both concentrations. For this frequency, an estimate of ϵ_{\perp} of the cell PDLC with 0.1 wt% of silicon dioxide gives the value $\epsilon_{\perp} \approx 11.6$ ($S = 1 \text{ cm}^2$, $d = 60 \mu\text{m}$), while the memory effect leads to a shift of this value to $\epsilon_{\perp} \approx 13.1$. The perpendicular ϵ_{\perp} component decreases both in the initial state and in the memory mode — 7.8 and 8.4,

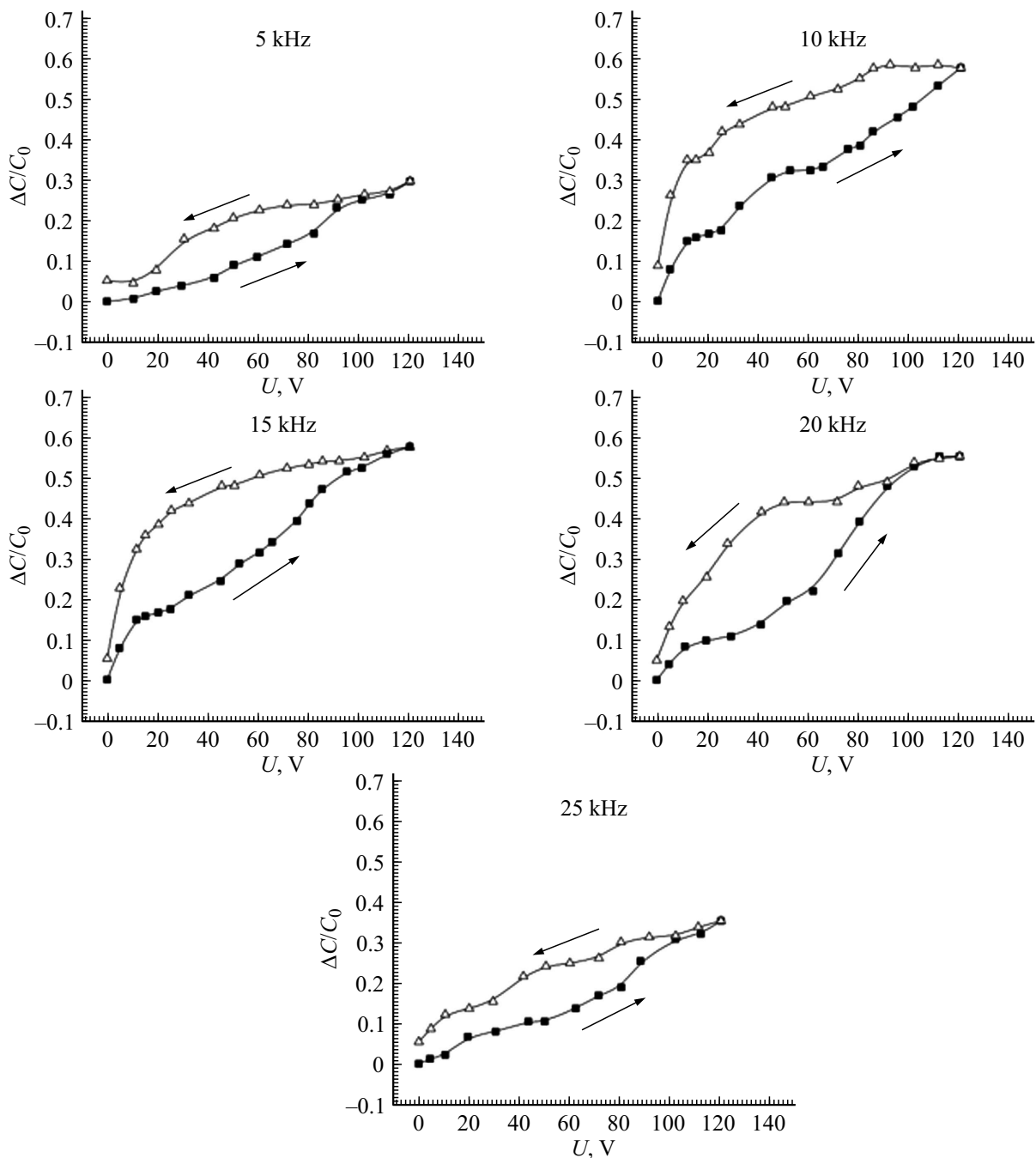


Figure 5. Volt-farad characteristics of the PDLC cell (1 wt% silicon dioxide) at generator frequencies of 5, 10, 15, 20 and 25 kHz.

respectively, with an increase of the concentration of silicon dioxide in the PDLC film to 1 wt%, which is close enough to the value of ε_{\perp} for pure undoped LC 5CB — 7.

The above-mentioned frequency dependence of the cell capacity seems to indicate a resonance in the nanoparticle system, which leads to an increase of the memory effect. Indeed, when voltage is applied to the LC cell, silicon oxide nanoparticles are aligned along the electric field due to the action of liquid crystal molecules. The structure of nanoparticles is preserved when the electric field is nulled and partially holds the LC molecules in the direction

perpendicular to the plates. The hysteresis value, as indicated above, depends on the frequency of the applied voltage and is maximum at 10 kHz, i.e. the number of LC molecules directed perpendicular to the plate and held in the structure of nanoparticles at this frequency is maximum. In this case, the structure of nanoparticles should also be the most stable. Obviously, this is due to the interaction of nanoparticles with each other and, consequently, mechanical resonance in a system of nanoparticles. Therefore, in our opinion, the increase of dielectric permittivity in the kHz region is attributable to the cellular structure formed in a

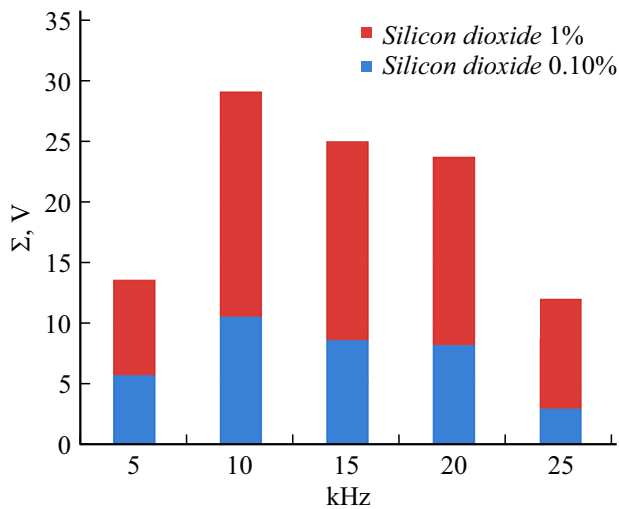


Figure 6. Diagram of hysteresis areas.

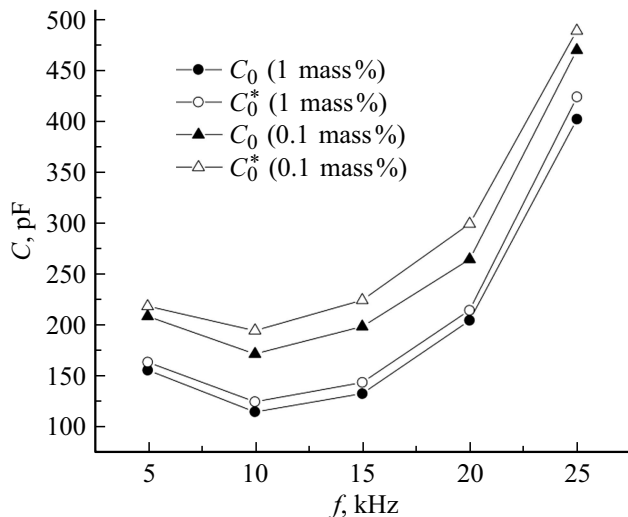


Figure 7. Frequency dependences of PDLC cell capacities.

constant field due to hydrogen bonds between nanoparticles and LC molecules.

Conclusions

As a result of an experimental study of the volt-farad characteristics of PDLC cells with silicon dioxide nanoparticles, a memory effect was detected, manifested in the hysteresis behavior of the capacitance of these cells. The memory effect in this case significantly depends on the frequency of the generator feeding the measuring bridge. The largest hysteresis area and the largest displacement of the cell capacity in the absence of an external field is observed at 10 kHz. Apparently, this is due to the fact that at this frequency a grid of silicon dioxide nanoparticles is created with the maximum number of cells containing LC molecules. In addition, the perpendicular component

of the dielectric permittivity has a pronounced dispersion over the entire studied frequency range with a minimum at a frequency of 10 kHz. An increase of the concentration of silicon dioxide nanoparticles from 0.1 to 1 wt% reduces the dielectric permittivity of the PDLC cell to values characteristic of an undoped LC. The obtained data can contribute to further research in the field of development of non-volatile nanostructured data storage systems.

Conflict of interest

The authors declare that they have no conflict of interest.

References

- [1] N. Nasir, H. Hong, M. Rehman, S. Kumar, Y. Seo. *RSC Adv.*, **10**, 32225 (2020). DOI: 10.1039/d0ra05911k
- [2] A.K. Jain, R.R. Deshmukh. *Liquid Crystals*, **46**, 1191 (2019). DOI: 10.1080/02678292.2018.1545264
- [3] J.V. Nimmy, S. Varanakkottu, S. Varghese. *Opt. Mater.*, **80**, 233 (2018). DOI: 10.1016/j.optmat.2018.05.003
- [4] R. Basu. *Phys. Rev. E*, **89**, 022508 (2014). DOI: 10.1103/PhysRevE.89.022508
- [5] R. Kempaiah, Y. Liu, Z. Nie, R. Basu. *Appl. Phys. Lett.*, **108**, 083105 (2018). DOI: 10.1063/1.4942593
- [6] V. Gdovinová, N. Tomasovicova, S.-Ch. Jengb, K. Zaku-tanská, P. Kulac, P. Kopcanskya. *J. Molecular Liquids*, **282**, 289 (2019). DOI: 10.1016/J.MOLLIQ.2019.03.001
- [7] S.P. Bardakhanov, A.I. Korchagin, N.K. Kuksanov, A.V. Lavrukhin, R.A. Salimov, S.N. Fadeev, V.V. Cherepkov. *DAN*, **409** (3), 320 (2006) (in Russian).
- [8] S.V. Kalashnikov, N.A. Romanov, A.V. Nomoev. *IOP, Conf. Ser.: Mater. Sci. Eng.*, **1198**, 012006 (2021). DOI: 10.1088/1757-899X/1198/1/012006
- [9] E.A. Konshina, D.P. Shcherbinin, M.A. Fedorov. *Workshop on Physics and Optics of Liquid Crystals and Composites Based on Them. Tutorial* (ITMO University, SPb, 2018)

Translated by Ego Translating